

ACCURACY ASSESSMENT OF THE URBAN LAND SURFACE TEMPERATURE CALCULATION BASED ON LANDSAT-8/OLI DATA (CASE STUDY: COYHAIQUE, CHILE)

Konstantin Verichev^a, Polina Mikhaylyukova^b, Alisa Salimova^c, Cristian Salazar^d and Manuel Carpio^{e,}
(manuel.carpio@ing.puc.cl*)*

(a) Faculty of Engineering Sciences, Universidad Austral de Chile, Valdivia, Chile

(b) Faculty of Geography, Lomonosov Moscow State University, Moscow, Russia

(c) School of Environment, Tsinghua University, Beijing, China

(d) Faculty of Economic and Administrative Sciences, Universidad Austral de Chile, Valdivia, Chile

(e) Department of Construction Engineering and Management, School of Engineering, Pontificia Universidad Católica de Chile, Santiago, Chile

ABSTRACT

The relationship between the values of the surface temperature retrieved from the Landsat-8/OLI satellite data and the values of the atmospheric temperature measured by NETAMO sensors in the urban environment of the Coyhaique city (Oct.2017-Sep.2018) was analyzed.

Based on the five satellite (one winter, one spring and three summer) images, the coefficient of the linear relationship determination between the two types of temperature was 0.85.

Index Terms—Chile, urban area, NETATMO, Landsat, remote sensing

1. INTRODUCTION

In recent years, extensive attention has been devoted to urban planning considering the urban heat island (UHI) effect and hydrothermal comfort for the city residents [1]–[4]. The ground-based observation and satellite imagery of the thermal spectral range were the main sources of the UHI analysis.

Some studies have observed an UHI effect using a variety of remote sensing technologies in Chile, especially in the capital city of Santiago, [5], [6]. Less attention has been paid to provincial cities with urban environment problems. For example, the capital of the Aysen region called Coyhaique (57,818 hab.) [7] that is

located in the southern part of Chile (Fig. 1), has high levels of an atmospheric pollution such as PM10 and PM 2.5 [8],[9]. An intensive furnace heating of the household in a winter period caused a high level of an atmospheric pollution that affects the ecosystem as well health and life quality of the city residents [10], [11].

In the conditions of the UHI effect, it is evident that during the winter, similar buildings (assuming identical architectural and construction parameters) located in the periphery of the city, have a higher demand for heating compare to buildings located on the center of the city, resulting in a higher energy consumption [2].

This work is the first stage in the study and modeling of the relationship of the energy consumption of houses and remote sensing data in small towns in the south of Chile. At the current stage, a large number of ground-based measurements were collected, which served as the basis for analyzing the accuracy of temperature values calculated using Landsat-8/OLI data.

The principal aim of this research is to reveal the relationship between the surface temperature obtained from the satellite images and atmospheric temperature obtained from the meteorological measurements in urban conditions of Coyhaique city.

2. METHODS AND DATA

2.1. Satellite data and surface temperature calculation method

To calculate the surface temperature of the city, 5 Landsat satellite images were used (Table 1).

Table 1. Satellite images used in study.

date	10.11.17	05.12.17	31.12.17	23.02.18	01.07.18
Sat.syst.	L.8 OLI				

Temperature calculation was performed in several stages: (i) Radiometric calibration; (ii) Atmospheric correction; (iii) Conversion from radiance to temperature.

We used band 10 of Landsat-8/OLI imagery because images of infrared range of 10.30 to 11.30 μm are less influenced by thermal emission than band 11 images [12].

Radiometric calibration is performed by using standard algorithm which is presented by satellite operator [13]–[15]:

$$CV_{R1} = DN * M_L + A_L \quad (1),$$

where: CV_{R1} – TOA spectral radiance ($\text{W}/(\text{m}^2\text{sr } \mu\text{m})$); M_L – Band-specific multiplicative rescaling factor from the metadata (RADIANCE_MULT_BAND_x, where x is the band number); A_L – Band-specific additive rescaling factor from the metadata (RADIANCE_ADD_BAND_x, where x is the band number); DN – Quantized and calibrated standard product pixel values. Values of M_L and A_L for the 10-th Landsat-8/OLI band is 0.0003342 and 0.1 respectively. **Atmospheric correction** of 10 band was based on algorithm from [13], [16]. The formula is:

$$CV_{R2} = \frac{CV_{R1} - L \uparrow}{\varepsilon \tau} - \frac{1 - \varepsilon}{\varepsilon} L \downarrow \quad (2),$$

where: CV_{R2} – corrected TOA spectral radiance ($\text{W}/(\text{m}^2\text{sr } \mu\text{m})$); $L \uparrow$ – effective bandpass upwelling radiance; $L \downarrow$ – effective bandpass downwelling radiance; τ – band average atmospheric transmission; ε – surface emissivity. $L \uparrow$, $L \downarrow$ and τ values were calculated for every image based on NASA Atmospheric Correction Parameter Calculator [17], where used information of: (i) date and time (UTC); (ii) latitude and longitude; (iii) standard model. Surface emissivity ε for different surface type was collected from different guides[6].

Conversion from radiance to temperature were based on formula [13]:

$$T = \frac{K_2}{\ln\left(\frac{K_1}{CV_{R2}} + 1\right)} \quad (3),$$

where: T – surface temperature [K]; CV_{R2} – corrected TOA spectral radiance; K_1 , K_2 – calibration coefficients for conversion from radiance to temperature from the metadata, values for Landsat-8/OLI band is 480.89 and 1201.14 respectively.

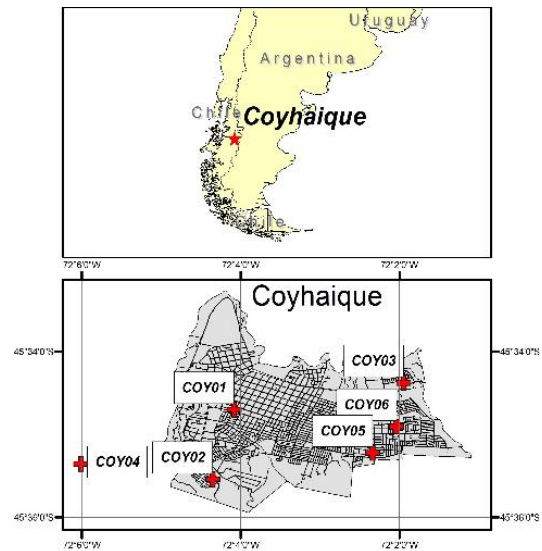


Fig. 1. Geographical location of the city and measurement points of NETATMO.

2.2. NETATMO meteorological data

Temperature measurements from 6 points in the city from Oct.2017 to Sep.2018. NETATMO sensors have a measurement accuracy of $\pm 0.5^{\circ}\text{C}$ [18], [19]. The distribution map of the meteorological measurement sites is shown on the Fig. 1. Sensors were set at 2 meters' height as standard meteorological measurements. All the 6 points COY01-COY06 were located in relatively densely build-up sectors in different parts of the city.

3. RESULTS AND DISCUSSION

The correlation between the atmospheric temperature measured by sensors and the land surface temperature values calculated from the five satellite images are represented in the Table 2.

Due to a complicated meteorological situation in a study area, only five satellite images (one from winter, one from spring and three from summer) were found cloudless a selected for a further research.

NETATMO sensors did not record the atmospheric temperature on all the dates. Therefore, on the basis of the 28 cases of parallel availability of the calculated land surface temperature and measured atmospheric temperature, a correlation graph was plotted between these temperature values (Fig. 2).

A rather high degree of correlation between temperatures values for different seasons was observed in the urban environment.

Using the obtained regression equation, it can be noted that in summer season, the surface temperature is much higher than the atmospheric temperature, due to the heating effect caused by solar radiation. Whereas in winter, the surface temperature values are lower than atmospheric, due to the cooling of the surface in winter.

The linear dependence can be also proved by the fact that all the images were taken during the anticyclone.

Table 2. Results of the retrieved land surface temperature (L.8) and the air temperature measured by sensors (N) [$^{\circ}\text{C}$].

		COY01	COY02	COY03	COY04	COY05	COY06
lon		-72,07	-72,07	-72,03	-72,10	-72,04	-72,03
lat		-45,58	-45,59	-45,57	-45,58	-45,59	-45,58
10.11.17	L.8	2,1	4,5	0,9	5,3	0,4	-1,1
	N	5,5	8,9	3	6,7	8,9	0,2
5.12.17	L.8	19,4	23,4	21,1	23,8	21,7	19,8
	N	17,7	15,5	19,1	17,4	18,6	18,9
31.12.17	L.8	12,1	17,1	13,9	17,5	14,1	10,8
	N	10,5	10	11,8	11,7	10,6	12,2
23.02.18	L.8	12,9	18,3	15,8	17,6	15,1	14,1
	N	-	11,4	13	11,7	11,5	11
01.07.18	L.8	-5,4	-0,2	-2	-2,1	-2,3	-4,2
	N	1,2	0,7	3,2	1,8	-	3

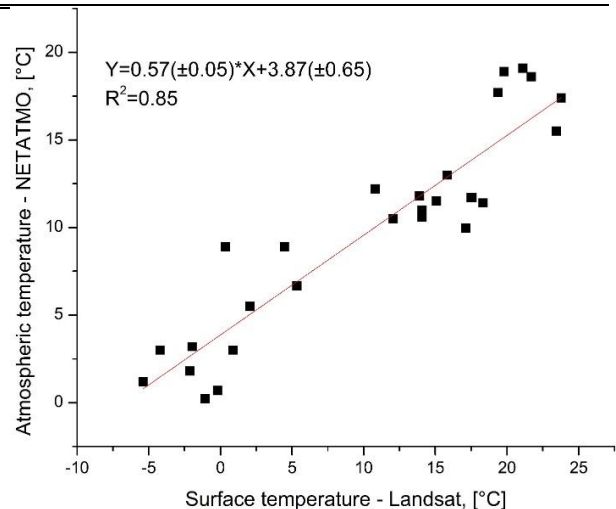


Fig. 2 Correlation between the land surface and atmospheric temperatures.

Based on the obtained dependence, the possibility of using satellite images for detailed thermal zonation of cities has been discovered.

The allocation of urban heat and cold centers is needed for a rational urban planning that ensures a comfort for urban citizens. A detailed microclimatic zoning has positive implications for the construction

management, choice of the building materials and architectural solutions that will minimize the energy costs for the households cooling or heating systems in different parts of the city.

However, the microclimatic zoning of UHI for the civil construction application needs a further research, modeling and analysis.

The derived regression equation can also be used to correct temperature values calculated by Landsat-8 / OLI channel 10. This calculation ensures an equal accuracy of the calculated values for analyzing the seasonal changes of the UHI.

4. CONCLUSIONS

A high degree of correlation between the temperature values obtained from satellite images and ground-based measurements in a small city was observed. This observation showed that satellite data can be used for the further spatial analysis of energy consumption by the households heating. These results have positive implications for increasing the efficiency of the energy use in cities of the southern Chile.

5. ACKNOWLEDGMENTS

This work was funded by the following research project: CONICYT FONDECYT 11160524.

6. REFERENCES

- [1] M. Nikolopoulou, N. Baker, and K. Steemers, "Thermal comfort in outdoor urban spaces: understanding the human parameter," *Sol. Energy*, vol. 70, no. 3, pp. 227–235, 2001.
- [2] A. L. Pisello, "State of the art on the development of cool coatings for buildings and cities," *Sol. Energy*, vol. 144, pp. 660–680, 2017.
- [3] B. Yang, T. Olofsson, G. Nair, and A. Kabanshi, "Outdoor thermal comfort under subarctic climate of north Sweden – A pilot study in Umeå," *Sustain. Cities Soc.*, vol. 28, pp. 387–397, 2017.
- [4] F. Salata, I. Golasi, D. Petitti, E. de Lieto Vollaro, M. Coppi, and A. de Lieto Vollaro, "Relating microclimate, human thermal comfort and health during heat waves: An analysis of heat island mitigation strategies through a case study in an urban outdoor environment," *Sustain. Cities Soc.*, vol. 30, pp. 79–96, 2017.
- [5] M. A. Peña, "Examination of the Land Surface Temperature Response for Santiago, Chile," *Photogramm. Eng. Remote Sens.*, vol. 75, no. 10, pp. 1191–1200, 2009.
- [6] M. A. Peña, "Relationships between remotely sensed surface parameters associated with the urban heat sink formation in Santiago, Chile," *Int. J. Remote Sens.*, vol. 29, no. 15, pp. 4385–4404, Aug. 2008.
- [7] INE, "INE AYSSEN - Instituto Nacional de Estadísticas." [Online]. Available: <http://www.ineaysen.cl/>. [Accessed: 09-Jan-2019].
- [8] C. Molina, R. Toro A, R. G. Morales S, C. Manzano, and M. A. Leiva-Guzmán, "Particulate matter in urban areas of south-central Chile exceeds air quality standards," *Air Qual. Atmos. Heal.*, vol. 10, no. 5, pp. 653–667, 2017.
- [9] WHO, "WHO." [Online]. Available: <https://www.who.int/search?query=coyhaique&page=1&pagesize=10&sortdir=desc&sort=relevance&default=AND&f.Countries.size=100&f.Lang.filter=en&f.RegionalSites.size=100&f.Topics.size=100&f.contentType.size=100&f.d.octype.size=101&facet.field=RegionalSites&face>. [Accessed: 06-Jan-2019].
- [10] EUROPE WHO, "Health effects of particulate matter," *World Heal. Organ. Reg. Off. Eur.*, 2013.
- [11] B. S. Sosa, A. Porta, J. E. Colman Lerner, R. Banda Noriega, and L. Massolo, "Human health risk due to variations in PM10-PM2.5 and associated PAHs levels," *Atmos. Environ.*, vol. 160, pp. 27–35, 2017.
- [12] USGS, "Landsat Missions: Imaging the Earth Since 1972," 2018. [Online]. Available: <https://landsat.usgs.gov/landsat-missions-timeline>. [Accessed: 09-Apr-2018].
- [13] The Yale Center for Earth Observation, "Converting Landsat TM and ETM+ thermal bands to temperature," 2010. [Online]. Available: <https://www.yale.edu/>. [Accessed: 07-Jan-2019].
- [14] Shashank Srinivasan, "Using data from the Landsat 8 TIRS instrument to estimate surface* temperature «geohackers," 2013. [Online]. Available: <https://geohackers.in/2013/08/using-data-from-the-landsat-8-tirs-instrument-to-estimate-surface-temperature/>. [Accessed: 07-Jan-2019].
- [15] USGS, "Using the USGS Landsat Level-1 Data Product | Landsat Missions," 2018. [Online]. Available: <https://landsat.usgs.gov/using-usgs-landsat-8-product>. [Accessed: 07-Jan-2019].
- [16] H. Yang, L. Zhang, L. Liu, and Q. Tong, "Algorithm of emissivity spectrum and temperature separation based on TASI data," *2011 IEEE Int. Geosci. Remote Sens. Symp.*, vol. 4619, no. 2008, pp. 1850–1853, 2011.
- [17] NASA, "Atmospheric Correction Parameter Calculator," 2019. [Online]. Available: <https://atmcorr.gsfc.nasa.gov/>. [Accessed: 07-Jan-2019].
- [18] D. Fenner, F. Meier, B. Bechtel, M. Otto, and D. Scherer, "Intra and inter 'local climate zone' variability of air temperature as observed by crowdsourced citizen weather stations in Berlin, Germany," *Meteorol. Zeitschrift*, vol. 26, no. 5, pp. 525–547, 2017.
- [19] F. Meier, D. Fenner, T. Grassmann, M. Otto, and D. Scherer, "Crowdsourcing air temperature from citizen weather stations for urban climate research," *Urban Clim.*, vol. 19, pp. 170–191, 2017.